15th International Symposium on Flow Visualization
June 25-28, 2012, Minsk, Belarus

MODELING OF TUNGSTEN ARMOUR DAMAGE UNDER ITER-LIKE TRANSIENT HEAT LOADS

B. BAZYLEV[1,c], R. A. PITTS[2]

[1]Karlsruhe Institute of Technology, IHM, P.O. Box 3640, 76021 Karlsruhe, Germany
[2]ITER Organization, Route de Vinon sur Verdon, 13115 Saint Paul Lez Durance, France

[c]Corresponding author: Tel.: +4972160824696; Fax: +4972160824874; Email: boris.bazylev@kit.edu

KEYWORDS:
Main subjects: plasma heat load, heat transfer, melting**,** armour damage, modeling, tokamak
Fluid: melt layer flow, shallow water, driving forces
Visualization method(s): Tecplot 360 package, ORIGIN 8.1

ABSTRACT: The second ITER divertor will be an all-tungsten variant of the first (CFC-tungsten) system to be installed for the non-active operation phases. However, tungsten melting and melt splashing during transients can lead to modifications of surface topology which may significantly decrease the lifetime of some regions of the divertor cassettes. Such melting will occur under the transient heat loads if leading edges are present on which plasma fluxes can impinge at nearly normal incidence. The work reported here uses the MEMOS code to investigate the consequences for W material damage as a result of plasma heat loads on vertical faces of misaligned leading edges between divertor cassettes due to downwards vertical displacement events expected on ITER.

INTRODUCTION. Tungsten (W) is now foreseen as most promising armour material for plasma facing components (PFCs) in the ITER divertor, baffle and the dome. Moreover, the second ITER divertor will be an all-tungsten (W) variant of the first system to be installed for non-active operation phases, which will use carbon fibre composite (CFC) in the high heat flux areas [1]. During the expected transients (disruptions, ELMs (Edge Localized Modes, and VDE (Vertical Displacement Events)) in ITER the armour will be exposed to hot plasma streams. The expected fluxes on the ITER divertor during transients are: Type I ELM energy fluxes of 0.5–6 MJ/m^2 during τ=0.3-0.6 ms, and thermal quench energy fluxes (disruptions) of 2-25 MJ/m^2, τ=1-5 ms [2]. The heat fluxes are expected to be so high that they can cause severe erosion of PFCs thereby limiting their lifetime. During intense transients the melting, melt motion, melt splashing and surface evaporation are seen as the main mechanisms of metallic armour erosion [3-9].

Tungsten melting and melt splashing during transients can lead to modifications of surface topology which may compromise subsequent plasma operation on or near damaged areas. Such melting will occur more readily under transient heat loads if leading edges are present on which plasma fluxes can impinge at nearly normal incidence. Whilst the divertor design is always such as to avoid or minimize the appearance of leading edges in the areas of high heat flux handling, a design which avoids all exposed edges in a system as large as the ITER divertor is difficult to realize when account is taken of the complex geometry, the accumulation of tolerances and the variation of plasma configurations.

The work reported here considers the consequences of varying degrees of component misalignment for W material damage under a range heat pulse transients (namely sets of energy density Q and reference duration τ) expected in ITER.

A particular area of concern are the edges present on either side of gaps between neighboring divertor cassettes in the upper baffle region of the outer (and to a lesser extent the inner) vertical target plates. The 20 mm gap between cassettes means that small misalignments, if present, are more exposed to heat fluxes at glancing angles of incidence. Downward vertical displacement events (VDE), can deliver very high parallel energy fluxes to the baffle regions and do so in a limiter configuration, in which magnetic field lines impact the baffle surfaces from both directions of attack. In the divertor strike point areas, cassette-to-cassette misalignments are protected by tilting the entire target at a slight angle, so that field lines cannot penetrate onto the side faces of monoblocks situated on plasma–facing units at the extremities of the cassettes. In the baffle area, the misalignment introduced by this tilt, although reduced by the curved geometry of the vertical target, may be problematic in the case of limiter-like plasmas at the thermal quench of a VDE. There is

some margin for the first divertor, used only in the non-active phases, since VDEs will not deposit the very highest energy densities expected during burning plasma operation. For the design of an all-W divertor to be used during the nuclear phase, however, it is important assess as quantitatively as possible the consequence for material damage of misaligned elements under the most severe transients. This paper provides some initial estimates to be used as a guide for more complete studies.

Simulations of W melting are performed using the MEMOS code, validated against plasma gun target erosion experiments for short transients and TEXTOR experiments for steady heat flux exposures [3-11]. The code runs take into account a realistic, but simplified description of the ITER divertor geometry, and assume that the gradient of the plasma pressure, and reactive force of evaporated material are the main drivers for acceleration of the melted tungsten.

Estimated heat loads on W monoblocks at the edges of neighbouring divertor cassettes in the worst expected ITER VDEs can exceed several hundred MJ/m^2 flowing parallel to the magnetic field for durations of a few ms [12]. Melt layer damage in this paper is thus estimated for single plasma loads in the range Q = 50 → 200 MJ/m^2, with reference pulse durations of τ = 4 ms, and edge misalignments up to several mm to cover the worst possible mechanical misalignment in the current divertor design. The influence of radiation originating from plasma shielding, formed by interaction of the evaporated material with incident plasma [13-15] on the different divertor components is also analyzed. The principal finding is that the most significant contributors to damage on misaligned edges are this radiation shielding, coupled with strong melt motion. The Tecplot 360 package and ORIGIN-PRO 8.1 are used for the result visualization.

SIMULATION IMPLICATIONS. A sketch of the simplified geometry of adjacent W monoblocks on each side of neighbouring ITER divertor cassettes is shown in Fig. 1. Plasma scenario calculations (e.g. with the DINA code package [16]) show that during a VDE impacting on the upper baffle region of the outer divertor target would deposit energy fluxes over a poloidal region of length up to ~40 cm, equivalent to ~10 monoblocks in the current first divertor design. The gradient of the heat load and other parameters (such as surface temperature, plasma pressure etc.) along the poloidal coordinate is thus not too large, especially for monoblocks in the centre of the plasma wetted area and so melt motion along the poloidal direction can be neglected. In this case, modeling of melt motion damage can be considerably simplified.

The real 3D geometry in Fig. 1 can be reduced to the 2D geometry shown in Fig.2 to perform more simple calculations using the 2D version of the code MEMOS. Here **G** indicates the monoblock lateral surface facing the plasma stream, **F** the shadowed lateral surface of the adjacent monoblock, **T** the monoblock top surface, which will intercept some part of the incident heat flux depending on the height **h** of the heated leading edge, **A** is the gap width between neighbouring cassettes and **b** is the distance from the monoblock corner to a selected point on the lateral surface.

Numerous earlier calculations of plasma shield formation under the impact of giant ELMs and disruptions have been performed using the FOREV-2 code [4,5,13-15]. These studies have revealed a number of key steps in the interaction process which are important for the damage simulations reported here:

1. The incoming plasma flux heats the surface up to high temperature such that significant evaporation occurs.
2. The evaporated material expands towards the incoming plasma and essentially screens the target surface from the plasma stream (so that direct heating by the plasma is reduced by a large factor).
3. Evaporated material is heated by the plasma up to rather high temperatures so that the plasma shielding layer becomes the source of intense radiation (at the level of several GW/m^2.
4. This intense radiation lasts for a slightly longer time than the plasma loads.
5. Typical plasma pressures in the plasma shield region are comparable with the pressure of the incident plasma stream and will be on the order of several bars for the intense VDE loads at near normal incidence considered here. The radiation from the plasma shielding heats the target surface and surrounding components and can cause significant damage even in shadowed regions.

Analysis of the plasma shielding formation leads to the development of the following physical model for use in the ITER misaligned edge damage simulations. A plasma stream with energy density Q heats the lateral target leading edge **h**. Tungsten evaporated from the heated area expands towards the plasma stream and is heated by the incident plasma stream up to ~10 eV. A plasma shield forms on the front surface of the leading edge. Part of the evaporated and heated tungsten flows onto the top surface **T**, generating a plasma shield with approximately the same plasma parameters as those for the layer protecting the front leading edge. Penetration of the heated plasma into the gap is insignificant and is

determined by the diffusion across toroidal magnetic field lines. As a result, the plasma pressure inside the gap is much lower than that in the vicinity of the leading edge. The plasma shielding generates radiation power densities of a few GW/m^2 which heat the surfaces **T**, **G** and **F**. Material evaporated from the lateral target surfaces expands into the vacuum inside the rather large volume of the gap. The density of this evaporated tungsten is assumed to decrease quickly and this rather cold tungsten vapor does not screen the lateral surface from the incoming radiation.

The plasma pressure along surface **F** is considered to be negligible, whilst the pressure along **G** falls according to a Gaussian law with half width P_G=0.1 cm from the irradiated edge: $p_G(b) = p_0 e\left(-(b/P_G)^2\right)$, with p_0 the plasma pressure in front of the leading edge at the top of the gap. Along the top surface **T** a Gaussian distribution is also assumed for the pressure, though now with a much larger half width: edge $p_T(x) = p_0 e\left(-(x/P_T)^2\right)$ with P_T = 6 cm. The heat loads on the lateral surfaces **F** and **G** are determined entirely by the radiation flux, S_{rad} from the shielding layer [5]. Assuming that the plasma layer in front of the edge surface is relatively optically thick and uniform along the gap, the radiation flux on the lateral surfaces at the position **b** may be estimated with the following expressions [4]:

$$S_G(b) = \frac{S_{rad} A^2}{2(A^2 + b^2)}, \quad S_F(b) = \frac{S_{rad} A^2}{2(A^2 + b^2)} \qquad (1)$$

The radiation flux along surface **T** exponentially decreases with characteristic length L_T =6 cm from the irradiated edge: $S_T(x) = S_{rad} e\left(-x/L_T\right)$.

Simulations are performed on the model 2D poloidal cross-section for several incident plasma heat loads assuming that the plasma pressure gradient force dominates over **jxB** forces so that the latter can be neglected (in the absence of halo and eddy currents – see below – the only **jxB** force which would act is that driven by the interaction of the incoming plasma stream current with the poloidal field and this is expected to be weak compared with the pressure gradient effect). A 2D heat transport equation with two boundary conditions at the moving vapor-liquid and liquid-solid interfaces describes the temperature inside the target. Temperature dependent thermo-physical data such as heat conductivity coefficients, heat capacity and pressure of saturated vapor are used [17-18]. The model of plasma shield formation used in MEMOS to account for the influence of evaporated material on surface heat loads is well developed and has been validated against experiments at plasma gun facilities [13].

RESULTS AND DISCUSSION OF MELT LAYER EROSION SIMULATIONS.

Simulations have been performed for the folowing scenarios
1) Q=50 MJ/m^2, S_{rad}=1 GW/m^2, p_0= 1.5 bar. 2) Q=100 MJ/m^2, S_{rad}=1.5 GW/m^2, p_0= 2.0 bar, 3) Q=150 MJ/m^2, S_{rad}=1.8 GW/m^2, p_0=2.5 bar, 4) Q=200 MJ/m^2, S_{rad}=3 GW/m^2, p_0= 4.0 bar and 5) Q=200 MJ/m^2, S_0=2 GW/m^2, p_0= 2.5 bar. In all cases, the plasma heat load is assumed to have rectangular shape and a duration of τ = 4 ms, roughly corresponding to the expected timescale for the VDE thermal quench on ITER. This assumption of a rectangular pulse is conservative, since the real time envelope of the heat load is expected to be more triangular. After the 4 ms pulse, the earlier FOREV-2 simulations indicate that the radiation flux can be assumed to fall exponentially according to the following expression: $S_T(t) = Se\left(-(t-\tau)/\tau_D\right)$ with τ_D=0.1τ . In the simulations an irradiated length of 1.5 cm from the corner along the lateral surfaces **G** and **F** is assumed, with 1.7 cm taken along the top surface **T.** The lengths chosen for the simulations correspond to the typical brush sizes.

In all five simulated cases, plasma loads at the misaligned leading edge are high enough to heat the tungsten up to temperatures above 4000 K, when significant evaporation occurs and plasma shields develop during the first few hundred □s in front of the leading edge **h**. Intense radiation from the plasma shielding heats lateral surfaces **G** and **F** up to high temperature, exceeding melting thresholds rather quickly and maintaining the temperature in the range 4000-5000 K throughout the duration of the plasma shield.. This leads to deep melting of both lateral surfaces and strong evaporation. The melt pool depth at the surface **F** increases from 210 μm up to 430 μm as the radiation loads increase from 1 - 4 GW/m^2 (Figs. 3-4). The thickness of evaporated tungsten increases correspondingly from 9 μm up to 112 μm.

Under the pressure of the incident plasma stream the evaporated tungsten is partly displaced into the gap along the lateral surface **G** and a plasma pressure gradient appears along this surface. This generates strong melt motion along the surface inside the gap from the irradiated leading edge. The velocity of such motion can achieve values on the order of m/s, but more typical values are 0.2-0.4 m/s. The melt motion produces rather deep craters along the irradiated leading edge, ranging between 50 μm for Q=50 MJ/m^2 to 170 μm for Q=200 MJ/m^2 (Figs. 5,7,9). Inside the gap at the edge of the irradiated area, mountains of melted material are formed with altitude ranging between 15 and 40 μm for the same range of heat flux densities. With increasing heat load, the strong W evaporation can decrease the height of this material accumulation (Figs. 5,7,9).

A practically uniform plasma shielding layer with low associated pressure gradient appears along the top surface **T**. As a result, melt layer motion along the surface is lower than for the case inside the gap. The maximum calculated crater depth is found near the monoblock corner and ranges between 31 μm for Q=50 MJ/m^2 and 135 μm for Q=200 MJ/m^2 (Figs. 6,8,10). At the edge of the irradiated area material accumulation occurs in the range 0 - 17 μm (Figs, 6,8,10).

These preliminary findings may be summarized in the following way: the total damage extent expected on the shadowed lateral surface **F** is determined by W evaporation due to the intense radiation fluxes originating from plasma shielding. On the lateral surface **G** facing the plasma stream, the damage occurs due to a combination of W evaporation due to intense radiation and melt motion generated by the high pressure gradient of plasma penetrating along the surface inside the gap from the plasma shielding formed at the leading edge. On the top surface **T** damage is determined by tungsten evaporation due to the plasma shield radiation and by melt motion driven by the pressure gradient of plasma being mostly displaced along the surface from the plasma shielding formed at the leading edge.

More accurate simulations would require knowledge of the real distributions of radiation from plasma shielding, the distribution of plasma pressure, the halo current density crossing the monoblock surfaces and the eddy current density generated inside the monoblock. The latter two currents would allow a proper estimation of the effect of **jxB** forces and hence to more realistic prediction of the possibility of melt splashing. Since the upper baffle area is not solicited in normal operation as a high power handling area, one of the principal concerns of these heavy transient interactions is the possibility that significant melt layer losses could be provoked by the VDE in the form of droplet splashing which may spread particulates to other areas of the divertor and hence present difficulties for subsequent plasma operations. Different splashing mechanisms must be included in further more precise simulations. Some of the necessary parameters can be obtained from 3D MHD simulations of plasma impact in the baffle regions.

CONCLUSIONS. A physical model based on the 2D code MEMOS, together with the results of existing work on plasma shield formation results has been developed for simulations of tungsten monoblock damage in the ITER divertor under conditions of high transient energy loading. Emphasis is placed in this paper on the upper baffle region of the vertical target and in the case of downward vertical displacement events.

The simulations demonstrate that the total material damage on the monoblock surfaces is determined by a combination of tungsten evaporation, caused by intense radiation from the plasma shielding effect and intense melt motion, generated by pressure gradients in the plasma which penetrates either along the surface inside the gap or is displaced along the surface from the plasma shield region formed at the leading edge.

More comprehensive and precise simulations will be required to investigate the influence of jxB forces which may arise as a result of halo and eddy currents appearing during VDE. Estimates of the likely melt splashing generated by different mechanisms such as Kelvin-Helmholtz and Rayleigh-Taylor instabilities should are also an important element to be considered by future simulations.

MODELING OF TUNGSTEN ARMOUR DAMAGE UNDER ITER-LIKE TRANSIENT HEAT LOADS

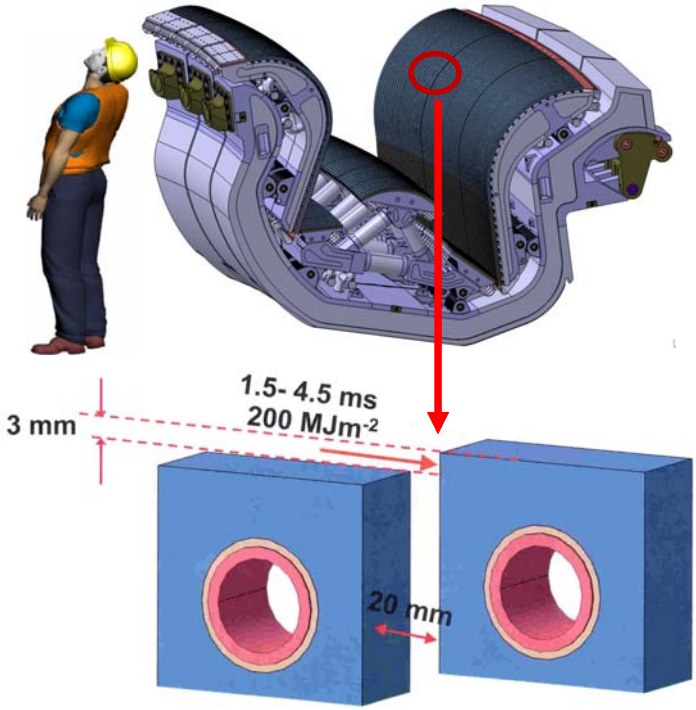

Fig. 1. Sketch of misaligned edge between monoblocks on sides of two neighbouring divertor cassettes

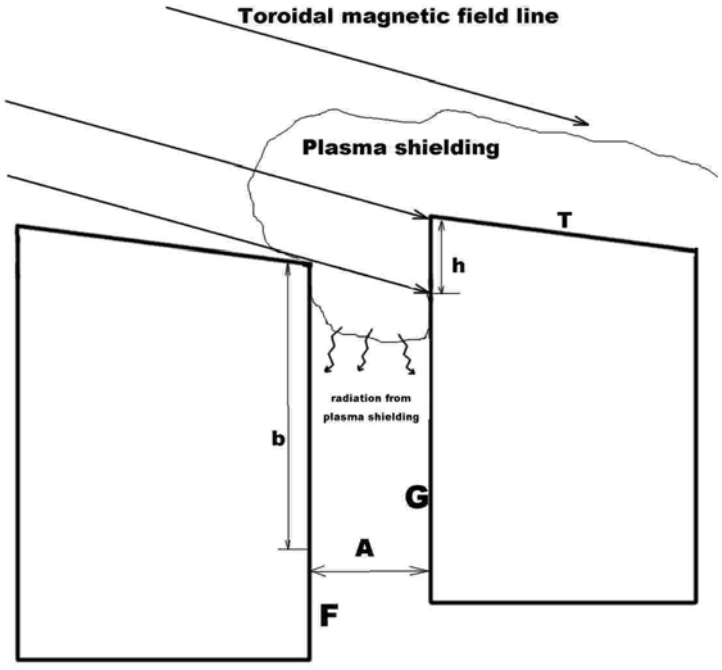

Fig. 2. Schematic of the simulation geometry

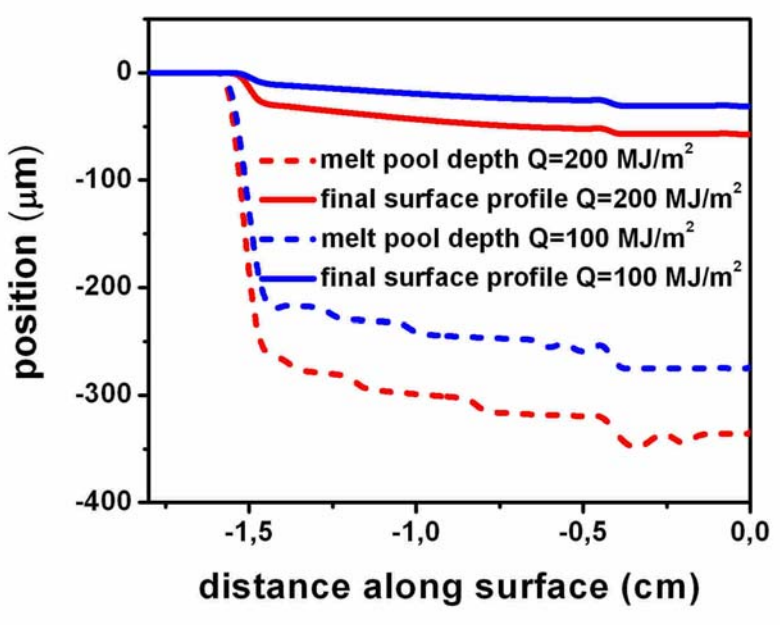

Fig.3. Final surface profile (caused by evaporation) and maximum melt pool depth along the lateral surface **F** (Fig. 2) for scenarios with τ =4 ms, Q=200 MJ/m^2 and 100 MJ/m^2 (corresponding to expected plasma shielding radiation fluxes of S_{rad}=2 GW/m^2 and 1.5 GW/m^2 respectively).

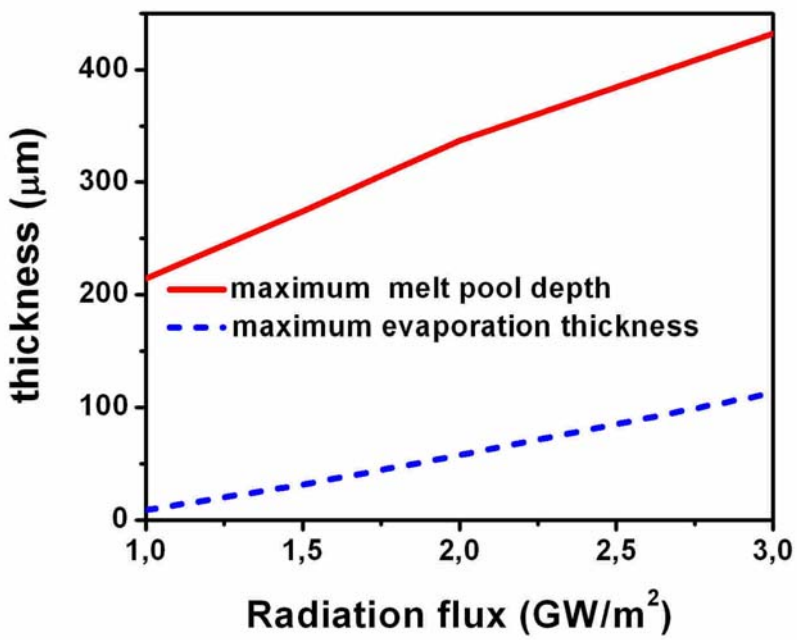

Fig. 4. . Dependence of maximum melt pool depth and average evaporation thickness on radiation heat loads for the lateral surface **F** (Fig. 2)

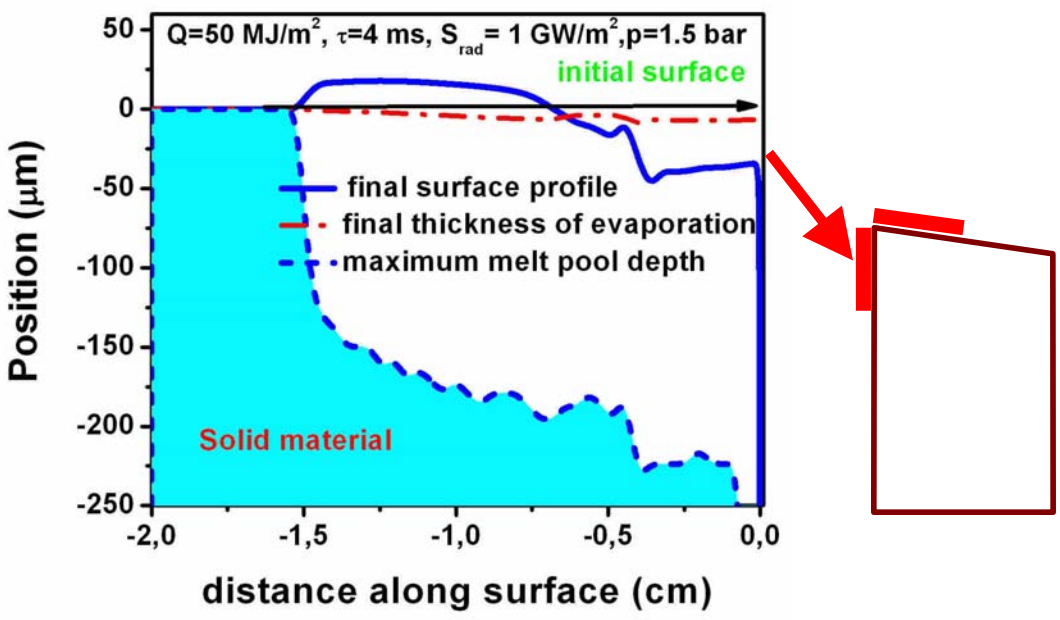

Fig.5. Final surface profile, maximum melt pool depth and evaporation profile along the lateral surface **G** (Fig. 2) for Q=50 MJ/m^2, τ =4 ms, plasma shielding radiation flux of S_{rad}=1 GW/m^2 and plasma pressure p=1.5 bar.

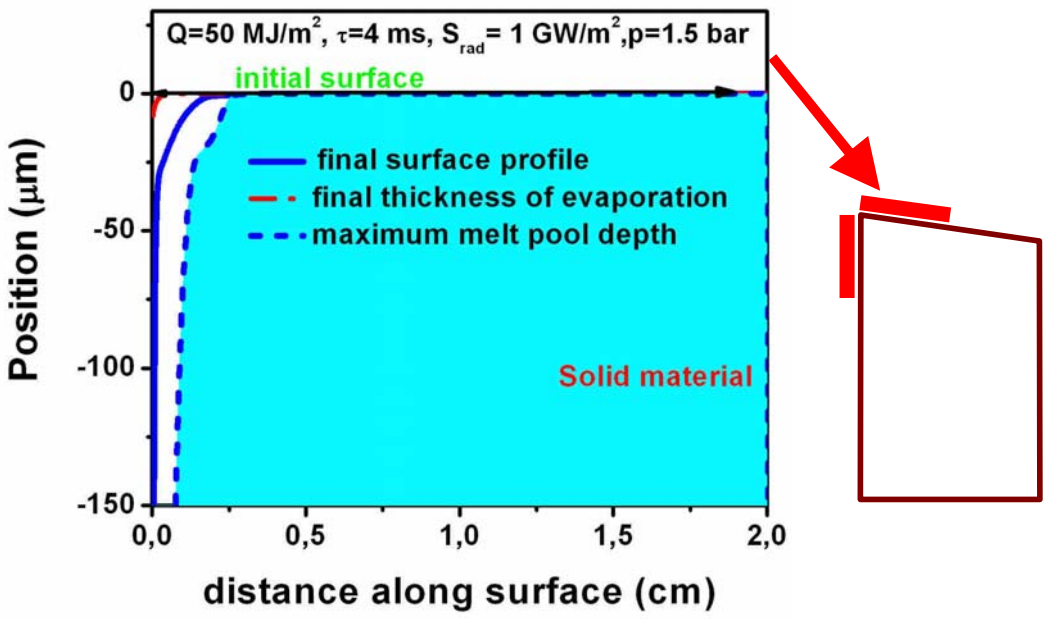

Fig. 6. Final surface profile, maximum melt pool depth and evaporation profile along the top surface **T** (Fig. 2) for Q=50 MJ/m^2, τ =4 ms, plasma shielding radiation flux of S_{rad}=1 GW/m^2 and plasma pressure p=1.5 bar.

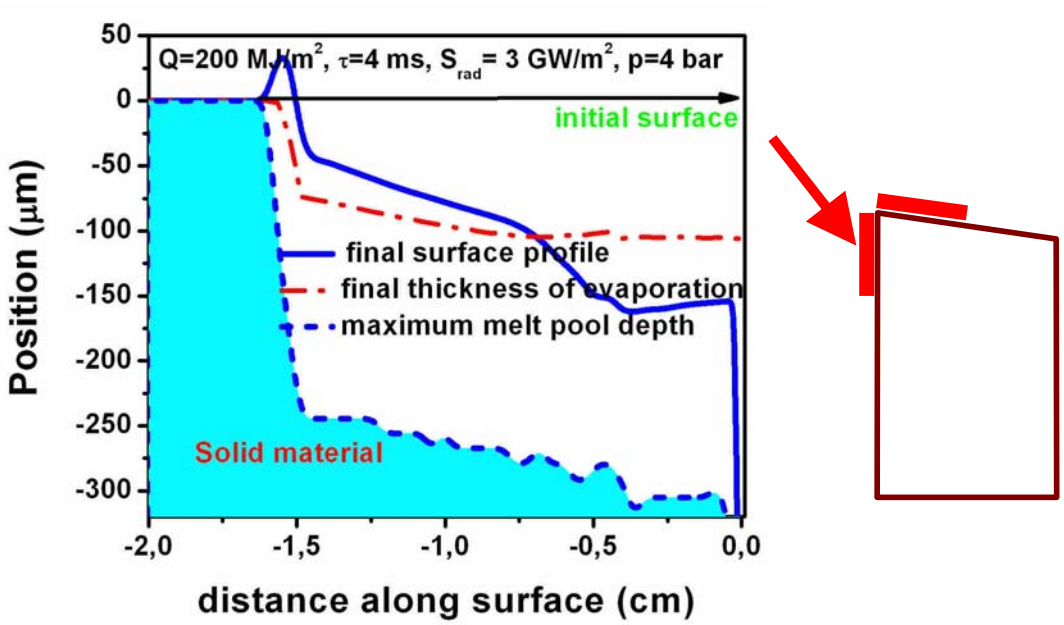

Fig. 7. Final surface profile, maximum melt pool depth and evaporation profile along the lateral surface **G** (Fig. 2) for Q=200 MJ/m^2, τ =4 ms, plasma shielding radiation flux of S_{rad}=3 GW/m^2 and plasma pressure p=4 bar.

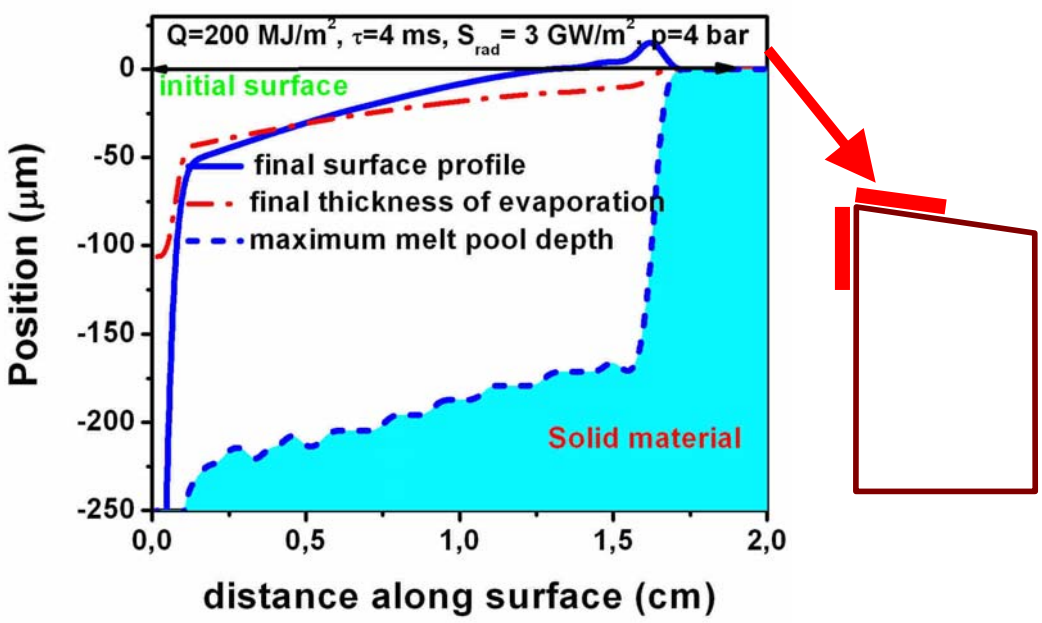

Fig. 8. Final surface profile, maximum melt pool depth and evaporation profile along the top surface **T** (Fig. 2) for Q=200 MJ/m^2, τ =4 ms, plasma shielding radiation flux of S_{rad}=3 GW/m^2 and plasma pressure p=4 bar

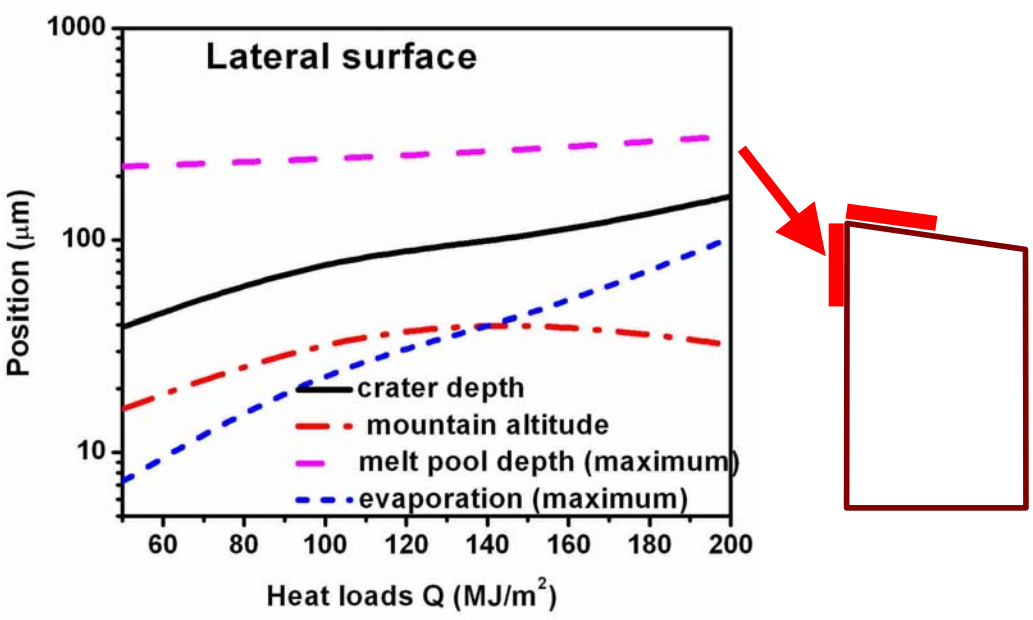

Fig. 9. Dependences of maximum crater depth, maximum mountain altitude, maximum melt pool depth, average evaporation thickness on plasma heat loads for the lateral surface **G** (Fig. 2)

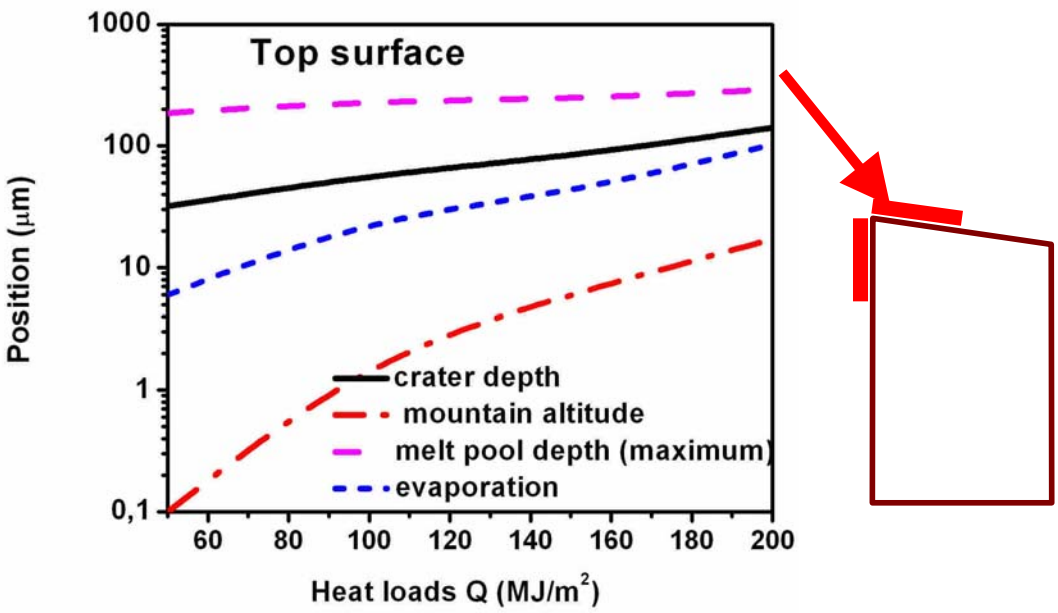

Fig. 10. Dependences of maximum crater depth, mountain altitude, maximum melt pool depth, average evaporation thickness on plasma heat loads for the top surface **T** (Fig. 2)

References

1. Pitts R.A. et al. *Status and physics basis of the ITER divertor*. Physica Scripta. 2009, **T138**, p.014001
2. Loarte A. et al. *Transient heat loads in current fusion experiments, extrapolation to ITER and consequences for its operation.* Physica Scripta 2007, **T128,** p. 222
3. Bazylev B., Wuerz H. *Melt layer erosion of metallic armour targets during off-normal events in tokamak.* J. Nucl. Mater. 2002, **307-311**, p. 69.
4. Bazylev B. et al. *Erosion of tungsten armour after multiple intense transient events in ITER.* J. Nucl. Mater. 2005, **337-339**, p. 766.
5. Bazylev B. et al. *Erosion of macrobrush tungsten armour after multiple intense transient events in ITER.* Fusion Eng. and Design. 2005, **75–79**, p. 407
6. Bazylev B. et al. *Melt damage simulations of W-macrobrush and divertor gaps after multiple transient events in ITER.* J. Nucl. Mater. 2007, **363-365,** p. 1011.
7. Bazylev B. et al. *Behaviour of melted tungsten plasma facing components under ITER-like transient heat loads: Simulations and experiments*. Fusion Eng. and Design. 2008 **83**, **Is. 7-9**, p. 1077.
8. Bazylev B. et al. *Experimental and theoretical investigation of droplet emission from tungsten melt layer.* Fusion Eng. and Design. 2009 **84, Is. 2-6,** p. 441.
9. Bazylev B. et al. *Experimental validation of 3D simulations of tungsten melts erosion under ITER-like transient loads*. J. Nucl. Mater. 2009, **390-391**, pp. 810.
10. Coenen J.W. et al. *Tungsten melt layer motion and splashing on castellated surfaces at the tokamak TEXTOR.* J. Nucl. Materials 2011, **415** (1), p. S78
11. Coenen J.W. et al. Analysis of tungsten melt-layer motion and splashing under tokamak conditions at TEXTOR. Nucl. Fusion 2011 **51** 083008 (11pp)
12. Pitts R.A. et al. *Physics basis and design of the ITER plasma-facing components.* J. Nucl. Mater. 2011**, 415**, **Is.1**, p. S957.
13. Wuerz H., et al. *A 2-D numerical Simulation of ITER-FEAT Disruptive Hot Plasma-Wall Interaction and Model Validation Against Disruption Simulation Experiments.* Fusion Science and Technology. 2001, **40**, p. 191.
14. H. Wuerz H. et al. *Erosion of ITER-FEAT vertical targets during off-normal events.* Fusion Eng. and Design. 2001, **56–57**, p. 349
15. Wuerz H. et al. *Macroscopic erosion of divertor and first wall armour in future tokamaks*. J. Nucl. Mater. 2002, **307–311**, p. 60
16. M. Sugihara M. et al. *Disruption scenarios, their mitigation and operation window in ITER*. Nucl. Fusion. 2007, **47,** p. 337
17. Touloukian Y.S. (ed). *Thermophysical Properties of Materials*, New York, 1970.
18. *Selected Values of Thermodynamic properties of the Elements*. American Society for Metals, Metal Park Ohio, 1973.